J Nanopart Res (2008) 10:1121–1128
DOI 10.1007/s11051-008-9359-2

FOCUS ON NANOFLUIDS

Production and characterization of carbon nano colloid via one-step electrochemical method

Doohyun Kim · Yujin Hwang · Seong Ir Cheong · Jae Keun Lee · Daeseung Hong · Seongyong Moon · Jung Eun Lee · Soo H. Kim

Received: 7 December 2007 / Accepted: 22 January 2008 / Published online: 16 February 2008

Abstract We present a one-step electrochemical method to produce water-based stable carbon nano colloid (CNC) without adding any surfactants at the room temperature. The physical, chemical, and thermal properties of CNC prepared were characterized by using various techniques, such as particle size analyzer, zeta potential meter, TEM, XRD, FT-IR, turbidity meter, viscometer, and transient hot-wire method. The average primary size of the suspended spherical-shaped nanoparticles in the CNC was found to be $\sim$15 nm in diameter. The thermal conductivity of CNC compared with that of water was observed to increase up to $\sim$14% with the CNC concentration of $\sim$4.2 wt%. The CNC prepared in this study was considerably stable over the period of 600 h. With the assistance of FT-IR spectroscopy analysis, we confirmed the presence of carboxyl group (i.e., O–H stretching (3,458 cm^{-1}) and C=O stretching (1,712 cm^{-1})) formed in the outer atomic layer of carbon nanoparticles, which (i) made the carbon particles hydrophilic and (ii) prevented the aggregation among primary nanoparticles by increasing the magnitude of zeta potential over the long period.

Keywords Colloid · Carbon nanoparticles · Oxidized graphite · Production · Characterization · Stability · Nanofluids

D. Kim · Y. Hwang · S. I. Cheong · J. K. Lee
Department of Mechanical Engineering, Pusan National University, San 30, Jangjeon-dong, Geumjung-gu, Busan 609-735, Korea

D. Hong · S. Moon
Institute of SamchangTsinghua Nano Application, N-BARO TECH CO., LTD, 974-1, Goyeon-Ri, Ungchon-Myon, Ulju-Gun, Ulsan 689-871, Korea

J. E. Lee
Industrial Liaison Innovation Cluster, Pusan National University, San 30, Jangjeon-dong, Geumjung-gu, Busan 609-735, Korea

S. H. Kim (✉)
Department of Nanosystem and Nanoprocess Engineering, Pusan National University, San 30, Jangjeon-dong, Geumjeong-gu, Busan 609-735, Korea
e-mail: sookim@pusan.ac.kr

Introduction

Nanotechnology is an important field at the crossroads of physics, engineering, and materials science. Especially, carbon nanostructures including carbon nanotube (CNT) and fullerene (C_{60}) have attracted much interest because of their potential applications in display, heat transfer media, fuel cell, secondary battery, shielding materials for electrostatics and electron wave, functional composite materials, and semiconductor and anti-wear materials. However, the applications of CNT and fullerene are limited because they are easily aggregated each other due to strong van der Waals attraction forces. To obtain

the stable dispersion of CNTs in an aqueous solution, an additive or chemical reagent is generally required (Jiang et al. 2003).

Hudson et al. (1997) and Peckett et al. (2000) prepared graphite particle-based nanofluid with the assistance of electrochemical oxidation method, where anodic erosion occurred at the surface of graphite electrode immersed in ethanoic acid, sulfuric acid, and deionized (DI) water. The size range of oxidized graphite particles obtained was 40–870 nm in diameter. Unlike those previous studies, we simply immersed electrodes into DI water without adding any surfactants in the combined electrochemical and sonochemical processes, and then we obtained stable carbon particle-based nanofluid with narrow primary size distribution, and also the production rate of our carbon nano colloid (CNC) fluid was reached at $\sim$1,400 g/h, which was $\sim$300 times larger amount than the colloidal production rate made by Peckett et al. (2000).

Here, we describe an electrochemical and sonochemical oxidation method to produce the water-based CNC with excellent stability. The morphology and size distribution of CNC prepared in this study were analyzed by using a TEM and a particle sizer (i.e., dynamic light scattering technique). Since the nanofluids such as CNC are the new engineering materials, we also measured the thermal conductivity and viscosity of CNC for their potential applications in heat transfer-enhanced systems. Turbidity analysis was also made to evaluate the colloidal stability of aqueous suspension. To investigate the stabilization mechanism of CNC prepared, FT-IR spectroscopy and zeta potential analysis were made.

Experimental

One-step electrochemical method for CNC preparation

High-density isotropic graphite was used as an anode, and a stainless steel plate was used as a cathode. The graphite anode used was 300 mm (W) $\times$ 500 mm (H) $\times$ 50 mm (D), and the perforated stainless steel plate cathode used was 300 mm (W) $\times$ 500 mm (H) $\times$ 3 mm (D). The distance between two electrodes immersed in a DI water bath was able to be varied from 1 to 100 mm at the current density of from 3 to 20 mA/cm^2. In the electrolysis process, the electric power applied to the electrodes was varied in multiple stages. (i) A constant voltage of 30 V, (ii) a constant current of 25 A, and then (iii) a constant current of 20 A were sequentially applied to the electrodes. Simultaneously, the colloidal solution was forcedly dispersed by an ultrasonicator, which was the flat-type ultrasonic equipment (Flexonic-1200-35/72/100G, Mirae Ultrasonic Tech., Korea). To prevent the aggregation of nanoparticles, the ultrasonicator was continuously operated at the power output of 1,000 W with the frequency of 100 ± 5 kHz during the production of CNC with the volume of $\sim$1 m^3. The combined electrochemical and sonochemical oxidation processes were kept for 30 days, and then the saturated concentration of CNC was found to be $\sim$0.4 wt%. We also monitored the electrical conductivity (σ) of the DI water using an electrical conductivity meter (LF11, SCHOTT) during the electrolysis process where the electrode was eroded to generate the CNC. We observed that the production of CNC was classified into three stages as follows: (i) the beginning stage of extremely low production rate of CNC (i.e., $\sigma < \sim 0.3$ dS/m) presumably due to initially high electrical resistivity of DI water ($\sim$50 kΩ m), (ii) the second stage of high production rate of CNC presumably due to the increase of the number concentration of electrolytes of both H^+ and OH^- ions generated by the continuous electrolysis process (i.e., $\sim 0.3 \leq \sigma < \sim 1.6$ dS/m), and (iii) the final stage of low production rate of CNC presumably due to the saturation of electrolytes (i.e., $\sim 1.6 \leq \sigma < \sim 1.7$ dS/m. Here, $\sim$1.7 dS/m was the maximum electrical conductivity observed in our electrochemical method.), and then the CNC generation was ceased when the electrode completely used up.

Characterization of physical, chemical, and thermal properties of CNC

The morphology of CNC was determined by a TEM analysis (JEMM 2011, Jeol). The FT-IR spectra were also measured by a Perkin Elmer Spectrum GX spectrometer in the wavelength range of 400–4,000 cm^{-1} with KBr pellet method under dry airflow. The high-resolution X-ray diffraction (XRD) patterns were obtained by a Philips X'pert Pro MRD. Particle size distribution and zeta potential of CNC were measured

by a dynamic light scattering and an electrophoretic light scattering (ELS-8000, Otsuka Electronics) technique, respectively. For evaluating the colloidal stability, the turbidity of CNC was measured as a function of sedimentation time with the assistance of nephelometer (2100AN, HACH). To measure the thermal conductivity of CNC, a transient hot-wire method was employed.

Teflon-coated platinum wire with the diameter of 76 μm and the length of 15 cm was used for thermal conductivity measurement based on the hot-wire method. Initially, the Teflon-coated platinum wire was immersed in the CNC, which was temperature controlled by a water bath. We applied constant voltage of 15 V (i.e., heat flux of ~110 W/m) to the electronic circuit of hot-wire system; the electric resistance of the Teflon-coated platinum wire increased with increasing the temperature of the wire. Here the voltage output was measured by an A/D converting system at the sampling rate of 20 times per second. The thermal conductivity of CNC was extracted from the slope of the rise in the wire's temperature against logarithmic time interval by the following equation (Nagasaka and Nagashima 1981).

$$k = \frac{q}{4\pi(T_2 - T_1)} \ln\left(\frac{t_2}{t_1}\right) \quad (1)$$

where k is the thermal conductivity of fluid and T is the temperature of the wire at time, t. In the series of hot-wire measurements, the average thermal conductivity of CNC with various weight concentrations at 25 °C was determined over five times repeated measurements. Here the measurement error in the thermal conductivity of CNC was less than ~1.5%.

The viscosity of CNC was measured by Ubbelohde viscometer (Capillary viscometer with viscoclock, SCHOTT).

Results and discussion

Morphology and particle size distribution measurements of CNC

Figure 1 shows the TEM image of CNC. One can see that the nanoparticles are spherical shape with the average diameter of ~15 nm. The size distribution of primary particles in the CNC was in-situ measured by using a dynamic light scattering measurement technique, which was presented in Fig. 2. The average size of primary particles was found to be ~18 nm with very narrow particle size distribution (i.e., standard deviation of ~1.16). It is presumably because the growth of particles in our one-step electrochemical method was suppressed by (i) the formation of functional groups on the surface of particles, which prevented the aggregation of resulting particles, which will be discussed in detail later, and also (ii) the presence of ultrasonication energy to separate the aggregated particles.

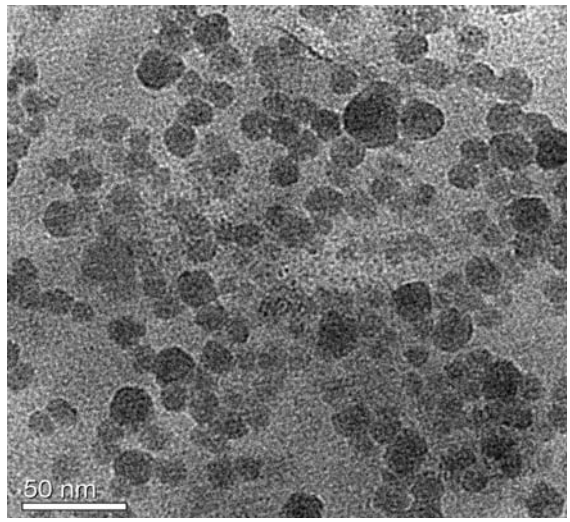

Fig. 1 TEM image of electrochemically produced carbon nano colloid (CNC)

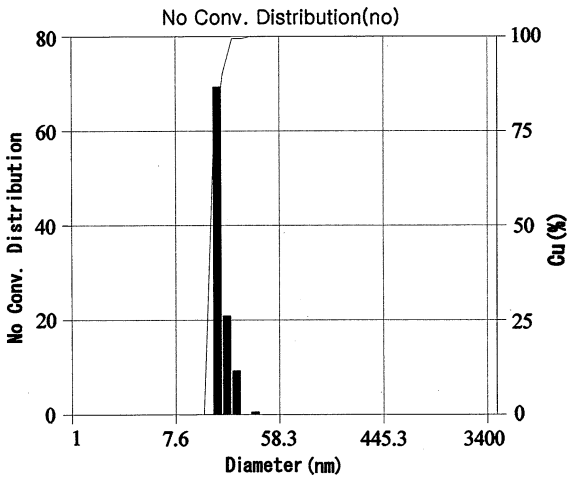

Fig. 2 Particle size distribution of CNC at 25 °C and pH = 2.3 measured by a dynamic light scattering technique

Measurement of thermophysical properties of CNC

To evaluate the heat transfer performance of CNC, we needed to measure its effective thermal conductivity and viscosity. Figure 3 shows the thermal conductivity enhancement of CNC compared with pure water. As the CNC concentration was increased from 0.4 wt% to 4.2 wt%, the thermal conductivity enhancement of CNC was observed to increase from ~2 to ~14%. Recently, Zhu et al. (2007) reported that the aqueous nanofluids with graphite nanoparticles enhanced the thermal conductivity of the base fluid by ~34% with the graphite colloid concentration of 2.0 vol%. However, for our CNC nanofluid with 2.4 vol% of carbon nanoparticles (i.e., 2.4 vol% of CNC can be calculated from ~4.2 wt% of CNC with the carbon density of 1.75 g/cm^3), we observed that the thermal conductivity of CNC was enhanced about ~14% compared with that of pure water. The discrepancy of thermal conductivity enhancement between Zhu et al.'s graphite nanofluid and our CNC nanofluid is presumably attributed to (i) the formation of non-crystalline structure of carbon in our CNC and (ii) the possible presence of oxide layer on the surface of carbon nanoparticles produced by the electrolysis process in our approach. To corroborate this, we performed the XRD analysis for both the bulk material of anode electrode (i.e., graphite) and the dried CNC particles. One can see that anode electrode material showed a major strong peak as a crystalline structure as seen in Fig. 4a, while dried CNC particles showed multiple peaks with relatively low intensity as seen in Fig. 4b, indicating that dried CNC particles are the mixture of polycrystalline and amorphous structures.

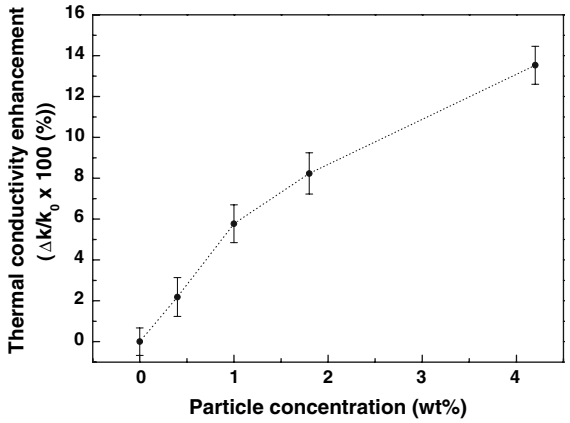

Fig. 3 Thermal conductivity enhancement of CNC as a function of particle concentration in CNC at 25 °C and pH = 2.3

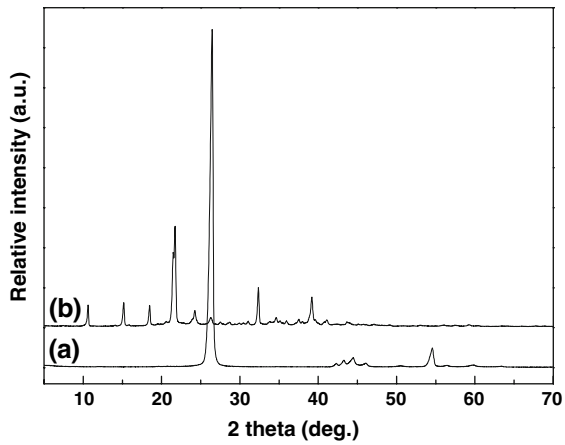

Fig. 4 XRD patterns of (a) the graphite particles sampled from anode electrode and (b) dried CNC particles

In the rheological study, the viscosity of CNC with various concentrations and temperatures was measured as shown in Fig. 5b. Some previous researches (e.g., Ding et al. 2006; He et al. 2007) showed that non-Newtonian behavior of nanofluid with shear thinning effect was appeared at the relatively low shear rate. In those works, the viscosity of suspension was decreased with increasing shear rate and finally reached to a constant value. In a shear thinning regime, the viscosity of suspension was observed to be larger than that of the base fluid by the order of 2–4. Unlike those works done by Ding et al. (2006) and He et al. (2007), another researches (Das et al. 2003; Prasher et al. 2006) presented that nanofluids had the behavior of Newtonian fluid. However, they did not present how the viscosity was varied at the lower shear rate (~50 s^{-1}). It is noted that nanofluid suspensions have shown controversial rheological behaviors between Newtonian and non-Newtonian flow regimes. We believe that the stability and dispersion states (i.e., agglomeration degree of primary particles and particle size distribution) also have a great influence on the viscosity characteristics of the suspension. These complicated behaviors of nanofluids have been investigated experimentally and theoretically by Larson (1999). However, we cannot find any information about the dispersion conditions for any of the previous researches. Therefore, it is

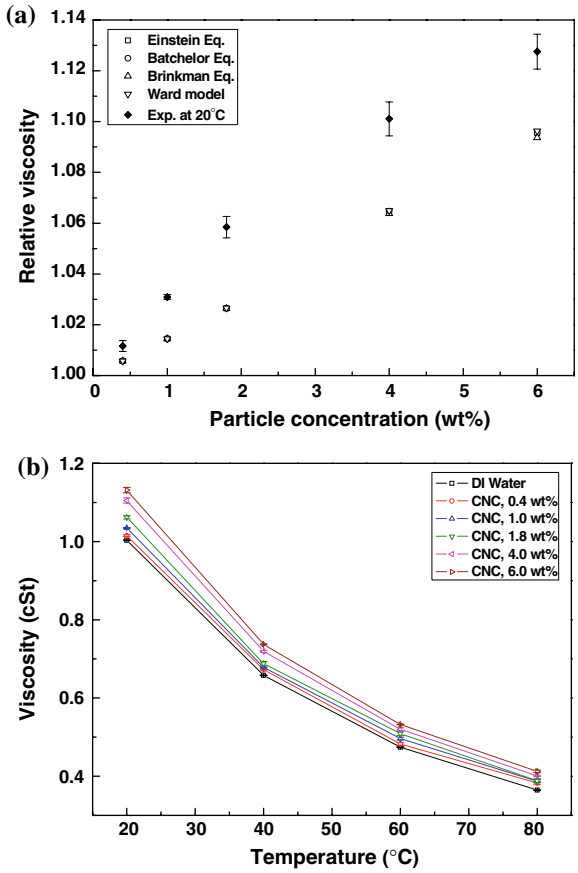

Fig. 5 (**a**) Comparison of the experimentally determined relative viscosity for CNC (pH = 2.3 and $T = 25$ °C) with theoretically determined viscosity and (**b**) the variation of the absolute viscosity of CNC with pH = 2.3 as a function of temperature

hard to compare those previous studies directly with our present approach at this point. Here, since the effective viscosity of the CNC compared with that of DI water (see Fig. 5b) in our approach was increased about less than ~15%, indicating that the CNC prepared in this study is categorized into Newtonian fluid. Therefore, we assumed the CNC as a Newtonian fluid so that we employed a capillary viscometer, which measured the time taken for a liquid level to pass through the constant length of capillary, and then Poiseuille equation is employed to determine the viscosity of nanofluids. The viscosity of CNC was decreased with increasing the fluid temperature, and simultaneously, it was increased with increasing the colloidal concentration. To check the validation of CNC's viscosity measured, we first compared the

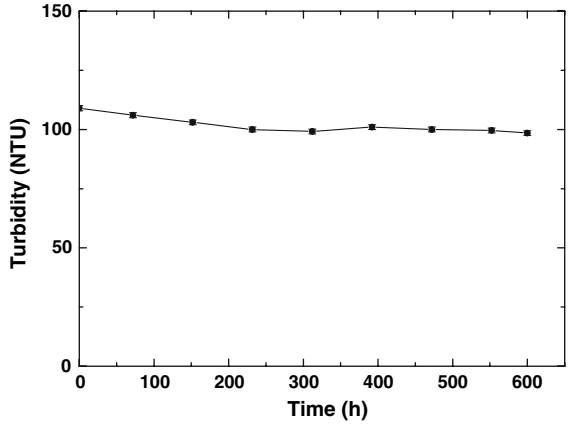

Fig. 6 Evolution of turbidity as a function of elapsed time for the 0.2 wt% CNC prepared at 25 °C and pH = 6.0

experimentally determined viscosity of CNC with the viscosity of general nanofluids calculated by several theoretical models suggested by Einstein, Batchelor, Brinkman, and Ward (Mansour et al. 2007; Avsec and Oblak 2007; Nguyen et al. 2008). Figure 5a shows that the experimentally determined viscosity of CNC was much higher than theoretically determined viscosity of nanofluids because those theoretical models did not account for nanoparticles' interactions and Brownian motion, which were occurred in our CNC nanofluids. Also, it is interesting to note that the viscosity of CNC with the concentration of even ~6 wt% was increased only ~15% compared with that of DI water. Since the increase of viscosity in nanofluids is generally resulted from anchoring between the aggregated particles in the nanofluids, this indirectly implies that the carbon nanoparticles in our CNC nanofluid were well separated by strong repulsion forces with even high concentration of nanoparticles (i.e., ~6 wt%).

Stability test of CNC

The stability of the ceramic suspension is generally determined by measuring the sediment volume as a function of time. However, this method is not suitable for our current CNC suspension because the CNC was too dark to detect the volume of sediment. Therefore the supernatant was analyzed in this approach for qualitatively evaluating the stability of CNC suspension by using a turbidity meter. In many

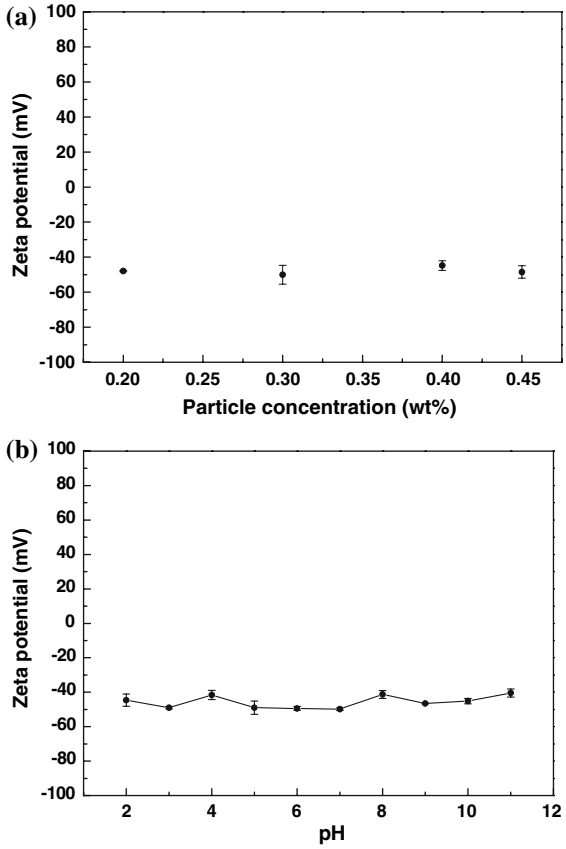

Fig. 7 The evolution of zeta potential as a function of (**a**) particle concentration and (**b**) pH for 0.2 wt% CNC at 25 °C

previous studies (Siffert et al. 1994; Den and Huang 2005; Janus et al. 2006), they employed the turbidity meter as an easy and reliable instrument to qualitatively evaluate the stability of nanofluids with the turbidity unit of approximately several hundreds of Nephelometric Turbidity Units (NTU). Since the turbidity of our resulting CNC was too dark (i.e., ~4.2 wt%), the turbidity of resulting CNC was out of detection range of our turbidity meter (2100AN, HACH). Therefore, prior to the turbidity measurement of the resulting CNC, we needed to sufficiently dilute it down to ~0.2 wt%, in which the CNC turbidity was then measurable (i.e., ~several hundreds NTU) and also it was observed to be very stable without any abrupt changes in the turbidity values for 600 h as seen in Fig. 6, indicating that the diluted CNC was very stable. Figure 7a shows the evolution of zeta potential of CNC as a function of CNC concentration, and Fig. 7b presents the zeta potential of 0.2 wt% CNC in the pH range from 2 to 11. One can see that the zeta potential of CNC is weakly dependent to the CNC concentration and pH values, indicating that our electrochemical oxidation method produced extremely stable carbon colloidal in water-based solution without adding any surfactants.

FT-IR spectrometer analysis of CNC

Now we turn our attention to investigate why CNC presented excellent stability without any surfactants. We performed FT-IR measurement for the original graphite electrode, the as-produced CNCs at pH = 2.3 and pH = 5.1, and the dried CNC nanoparticles. The FT-IR spectrum of the original graphite electrode prior to oxidation (i.e., spectrum (a) in Fig. 8) shows no significant bands except the weak absorption band at 1,697 cm^{-1} probably owing to impurities in the potassium bromide. Spectra (b) and (c) in Fig. 8 show the original CNC prepared at different pHs. Both spectra (b) and (c) similarly show the absorption bands at 3,367 and 1,639 cm^{-1}. Spectrum (d) in Fig. 8 presents the carbon nanoparticles, which were dried at 100 °C for 24 h. The strong transmittance signals appeared at 3,458, 1,712, 1,252, and 1,450 cm^{-1} are occurred due to O–H, C=O, C–O stretching, and O–H bending, respectively. Another strong band at 1,632 cm^{-1} is presumably occurred due to the C=C stretching of graphite. The border and strong peak from 2,300 to 3,500 cm^{-1} show the O–H stretching due to the presence of hydroxyl group, and

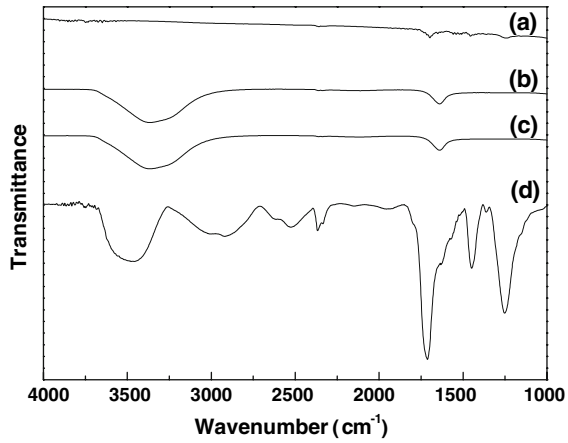

Fig. 8 FT-IR spectra of (a) the original graphite electrode, (b) electrochemically produced CNC with pH = 2.3, (c) CNC with pH = 5.1, and (d) dried CNC under 100 °C for 24 h

also the strong peak of 1,712 cm^{-1} shows the presence of carbonyl group. The carboxyl group combined with hydroxyl and carbonyl group are known as hydrophilic functional groups. We believe that the formation of hydrophilic functional groups on the surface of the carbon nanoparticles eventually resulted in the induction of strong repulsion forces among the primary carbon nanoparticles corroborated by zeta potential measurement (see Fig. 7) so that CNC nanofluids prepared in this study become stable for a long time period.

Possible mechanism of the formation of stable CNC

The functional groups such as carbonyl, hydroxyl, and carboxyl group were formed on surface of carbon nanoparticles verified by FT-IR analysis. A schematic representation of the graphite surface oxides was presented in Fig. 9. In the graphite structure, each carbon atom is covalently bonded to other carbon atoms so that they form flat sheet-like sequential hexagonal structures. However, the parallel flat sheets of hexagonal-structured carbon atoms are weakly bonded together by van der Waals attraction forces, implying that the parallel carbon flat sheets are easy to split by relatively weak external forces, and also other functional groups can easily enter between the graphite flat sheets (Kinoshita 1988).

On the basis of graphite structures, we describe the mechanism of the formation of stable CNC as seen in Fig. 10, which presents the schematic of CNC production process in the electrochemical and sonochemical

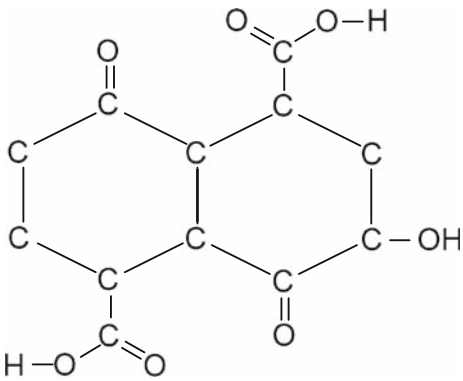

Fig. 9 The functional groups of graphite surface in the electrochemical oxidization process

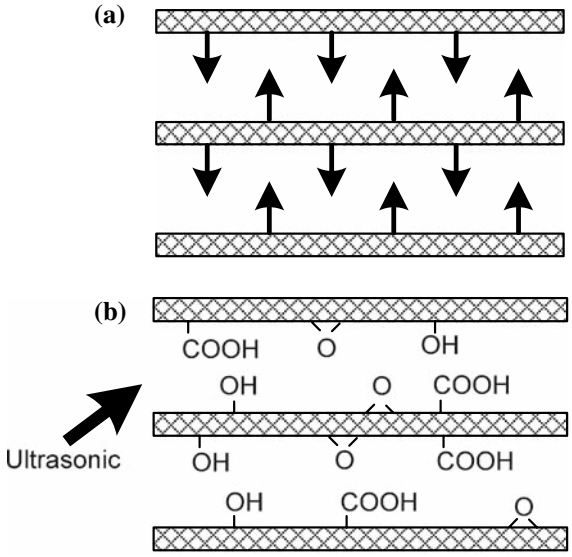

Fig. 10 The schematic of CNC production process in the electrochemical and sonochemical oxidization. (**a**) van der Waals attraction forces acting between the stacked layers in graphite and (**b**) functional groups-induced repulsion forces acting between the stacked layer in graphite

oxidization. Initially, the stacked layers of the graphite at the electrodes were bonded together by van der Waals attraction force (see Fig. 10a). During the electrochemical oxidization in the water, an anion (OH^-) formed from the cathode with the excess of electrons moved toward the anode with the deficit of electrons. At the anode, the electrons were removed at the surface of carbon nanoparticles, and simultaneously, the oxidation process was occurred. Furthermore, the ultrasonic treatment during the electrochemical process added cavitation energy on the surface of carbon nanoparticles for enhancing the dispersity. Since the combined oxidation and cavitation energy were imposed on the surface of carbon in the electrochemical process, the magnitude of repulsion forces formed between the stacked layers get larger than that of van der Waals attraction forces between the layers as depicted in Fig. 10b so that the resulting CNC nanofluid is able to maintain its stability as long as the hydrophilic functional groups exist.

Conclusions

With the assistance of a one-step electrochemical oxidization method, the ultra stable aqueous CNC

solution was successfully produced without adding any surfactants in this study. Various characterization techniques were employed to measure the physical, chemical, and thermal properties of the CNC by using TEM, XRD, particle sizer, FT-IR, zeta meter, transient hot wire, and viscometer. We found that the formation of the hydrophilic functional groups on the surface of carbon nanoparticles in the CNC solution, which eventually resulted in the excellent stability of the resulting CNC suspension in DI water. As a result of stability test, we confirmed that CNC is well dispersed in the DI water over a long time period up to $\sim$600 h. Also, the thermal conductivity of the CNC prepared with the initial concentration of $\sim$4.2 wt% was enhanced $\sim$14% compared with the thermal conductivity of pure water.

Acknowledgments This work was supported by grant no. 10026688 from the Advanced Technology Center Project of Ministry of Commerce, Industry and Energy.

References

Avsec J, Oblak M (2007) The calculation of thermal conductivity, viscosity and thermodynamic properties for nanofluids on the basis of statistical nanomechanics. Int J Heat Mass Transf 50:4331–4341

Das SK, Putra N, Roetzel W (2003) Pool boiling characteristics of nano-fluids. Int J Heat Mass Transf 46:851–862

Den W, Huang C (2005) Electrocoagulation for removal of silica nano-particles from chemical-mechanical-planarization wastewater. Colloids Surf A 254:81–89

Ding Y, Alias H, Wen D, Williams RA (2006) Heat transfer of aqueous suspensions of carbon nanotubes (CNT nanofluids). Int J Heat Mass Transf 49:240–250

He Y, Jin Y, Chen H, Ding Y, Chang D, Lu H (2007) Heat transfer and flow behaviour of aqueous suspensions of TiO_2 nanoparticles (nanofluids) flowing upward through a vertical pipe. Int J Heat Mass Transf 50:2272–2281

Hudson MJ, Hunter-Fujita FR, Peckett JW, Smith PM (1997) Electrochemically prepared colloidal, oxidized graphite. J Mater Chem 7(2):301–305

Janus M, Inagaki M, Tryba B, Toyoda M, Morawski AW (2006) Carbon-modified TiO_2 photocatalyst by ethanol carbonization. Appl Catal B Environ 63:272–276

Jiang L, Gao L, Sun J (2003) Production of aqueous colloidal dispersions of carbon nanotubes. J Colloid Interface Sci 260:89–94

Kinoshita K (1988) Carbon, electrochemical and physicochemical properties. John Wiley & Sons, Inc., NY

Larson RG (1999) The structure and rheology of complex fluids. Oxford University Press, Inc., NY

Mansour RB, Galanis N, Nguyen CT (2007) Effect of uncertainties in physical properties on forced convection heat transfer with nanofluids. Appl Therm Eng 27:240–249

Nagasaka Y, Nagashima A (1981) Absolute measurement of the thermal conductivity of electrically conducting liquids by the transient hot-wire method. J Phys E Sci Instrum 14:1435–1440

Nguyen CT, Desgranges F, Galanis N, Roy G, Mare T, Boucher S, Mintsa HA (2008) Viscosity data for Al_2O_3-water nanofluid-hysteresis: is heat transfer enhancement using nanofluids reliable? Int J Therm Sci 47:103–111

Peckett JW, Trens P, Gougeon RD, Poppl A, Harris RK, Hudson MJ (2000) Electrochemically oxidized graphite. Characterisation and some ion exchange properties. Carbon 38: 345–353

Prasher R, Song D, Wang J, Phelan P (2006) Measurements of nanofluid viscosity and its implications for thermal applications. Appl Phys Lett 89:133108

Siffert B, Jada A, Eleli-Letsango J (1994) Stability calculations of TiO_2 nonaqueous suspensions: thickness of the electrical double layer. J Colloid Interface Sci 167:281–286

Zhu H, Zhang C, Tang Y, Wang J, Ren B, Yin Y (2007) Preparation and thermal conductivity of suspensions of graphite nanoparticles. Carbon 45:203–228